RSC Advances

ROYAL SOCIETY OF CHEMISTRY

www.rsc.org/advances

Graphical Abstract

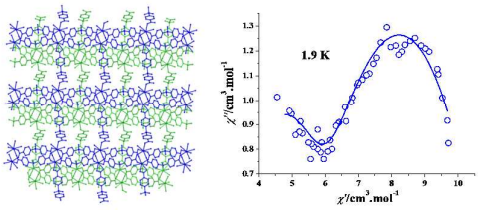

An entangled Dy(III) MOF with both polyrotaxane and polycatenane features was prepared, displaying two-step magnetic relaxation processes.

Journal Name

RSCPublishing

COMMUNICATION

Cite this: DOI: 10.1039/x0xx00000x

A 2D→2D polyrotaxane lanthanide–organic framework showing field-induced single-molecule magnet behaviour†

Received 00th January 2014,
Accepted 00th January 2014

DOI: 10.1039/x0xx00000x

www.rsc.org/

Cai-Ming Liu,*[a] De-Qing Zhang[a] and Dao-Ben Zhu[a]

The hydrothermal reaction of 4,4'-dicarboxybiphenyl sulfone and dysprosium(III) nitrate in the presence of *L*-histidine yielded the first 2D→2D polyrotaxane lanthanide–organic framework, which possesses both polyrotaxane and polycatenane topology features. Magnetic investigations indicated that it is a field-induced single-molecule magnet with two-step magnetic relaxation processes.

Polyrotaxane metal–organic frameworks(PMOFs), which belong to a special class of entangled networks constructed by insertion of linear rods through loops from the neighbouring net, have attracted considerable ongoing attention for their topological aesthetics and their potential for a variety of applications.[1] The main strategy for the assembly of the PMOFs is adopting mixed ligands with flexible and long rigid characteristics: the conformationally flexible ligand is able to generate the loop, while the long rigid ligand acts as the rod, penetrating through the flexible loops. Furthermore, some PMOF examples are based on only one semi-rigid ligand. To date, many fascinating PMOFs, including 1D→1D, 1D→2D, 2D→2D, 2D→3D and 2D/3D have been reported,[1g] however, most of them are transition metal complexes, the construction of polyrotaxane lanthanide–organic frameworks remains a great challenge, the difficulty maybe is that the lanthanide ions generally possess larger ionic radii and higher coordination numbers with respect to the transition metal ions.

On the other hand, with large magnetic moments and remarkable magnetic anisotropy, the lanthanide ions play an important role in the assembly of single-molecule magnets (SMMs), because both large spin ground state (*S*) and negative uniaxial magnetic anisotropy (*D*) are prerequisites for an SMM.[2] The SMMs show superparamagnet-like behaviours below the blocking temperature (T_B), having become the research focus due to their potential applications in high-density information storage, quantum computer and spintronics.[2,3] Most of SMMs are discrete cluster complexes or single-ion compounds. Notably, the energy barrier of the Ln-SMMs mainly originates from the single-ion anisotropy, the reason is that the effectively shielded 4f electrons often result in the magnetic exchange interaction between lanthanide ions to be very weak. Therefore, the SMM behaviours should also be observed in the MOF systems. However, the lanthanide–organic framework SMMs are still at an early stage of growth, only a few such examples have been documented in the literature.[4]

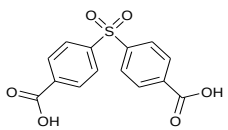

Scheme 1. H_2L ligand.

We also interested in the lanthanide based SMMs[5] and lanthanide–organic frameworks.[6] Recently, we chose the semi-rigid ligand, 4,4'-dicarboxybiphenyl sulfone (H_2L, Scheme 1), to synthesize lanthanide–organic frameworks. Herein we describe a novel Dy(III) PMOF, $[Dy_2L_2(H_2O)_5]_n$(**1**), which shows an interesting 2D→2D entangled network with both polyrotaxane and polycatenane features, and their loop and rod elements are composed of the same V-shape dicarboxylate ligand. Strikingly, unlike the known transition metal PMOFs, this complex displays field-induced single-molecule magnet properties.

Complex **1** was obtained as slight-grey plates in 25% yield by a hydrothermal reaction.‡ A mixture of H_2L (0.6 mmol), Dy_2O_3 (0.3 mmol) and *L*-histidine (0.3 mmol) in 10 mL water was sonicated for 10 min, then transferred to a 20 mL Teflon-lined stainless steel bomb and kept at 130 °C under autogenous pressure for 3 days. Surprisingly, although *L*-histidine is not incorporated into the structure of **1**, it plays a critical role in the formation of **1**, because the absence of *L*-histidine in the reaction mixture could not yield any crystalline products. Thermogravimetric analysis (TGA) of the polycrystalline samples revealed that complex **1** starts to lose hydrate molecules at about 80 ºC, and the loss of total five water molecules is completed at 210 ºC (calcd 6.78%, found 6.8%) (Fig. S1). Additionally, the following weight loss of 4.8% till 480 °C

corresponds to the loss of four oxygen atoms from two sulfone groups of two L^{2-} ligands (calcd 4.82%, found 4.8%). After that, the other parts of the L^{2-} ligand begin to decompose quickly, and the remaining framework collapses.

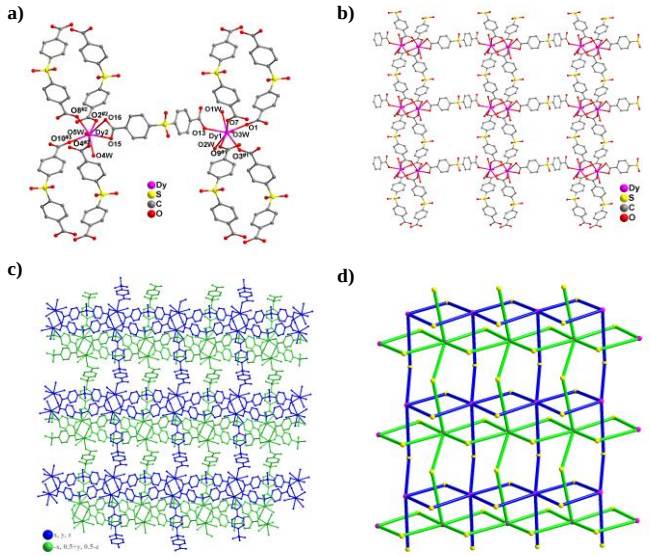

Fig. 1. (a) Coordination environment of Dy(III) atoms in **1**(#1 x, −1+y, z; #2 1+x, y, z; #3 1+x, 1−y, z), hydrogen atoms were omitted for clarity; (b) the sheet-like structure of **1**; (c) the interlocked nets in **1**; and (d) schematic view of the topology of **1**.

The crystal structure of **1**§ exhibits a 2D polyrotaxane network composed of the $Dy(III)_2$ dinuclear cluster nodes, L^{2-} bridging ligands, and hydrate terminal ligands (Fig. 1). There are two crystallographic independent dysprosium (III) atoms: the Dy1 atom is eight coordinated, completed by five O atoms from five L^{2-} ligands and three O atoms of the terminal hydrate molecules, generating a [DyO_8] coordination polyhedron. The Dy2 atom also has a [DyO_8] coordination geometry but with six carboxylato O atoms from five L^{2-} ligands and two O atoms from two terminal hydrate molecules. Generally, the eight-coordinate polyhedron conformations can be judged by the creased angles of two approximate square planes: the corresponding angles are 0° and 0° for a square antiprism, 0° and 21.8° for a bicapped trigonal prism, and 29.5° and 29.5° for a dodecahedron.[7] For the Dy1 atom, the two approximate square planes defined by O13−O2w−O3w−O1w and $O1-O7-O9^{\#1}-O3^{\#1}$ ($^{\#1}$ x, −1+y, z) are creased about the respective diagonals O13−O3w and $O1-O9^{\#1}$ with angles of 3.8° and 3.4°. Therefore, the polyhedron defined by the Dy1 atom and its bound atoms can be best described as a distorted square antiprism geometry (Fig. S2). For the Dy2 atom, the creased angles of two approximate square faces defined by $O8^{\#2}-O10^{\#3}-O4^{\#3}-O2^{\#2}$ ($^{\#2}$ 1+x, y, z; $^{\#3}$ 1+x, 1−y, z) and O4w−O5w−O16−O15 about the respective diagonals $O8^{\#2}-O4^{\#3}$ and O4w−O16 are 0.3° and 22.4°, so the Dy2 atom shows a distorted bicapped trigonal prism coordination polyhedron (Fig. S2). The Dy–O bond lengths (average 2.383(5) and 2.381(5) Å for the Dy1 and Dy2 atoms, respectively) are in the normal range.[2]

It is noteworthy that the L^{2-} ligands in **1** coordinate to the Dy(III) atoms with two modes [Scheme S1(a) and (b)]: in the former mode, the carboxylato group in one side links to the Dy1 atom with the monodentate mode whereas the carboxylato group in the other side connects with the Dy2 atom using the chelating mode, such a ligand works as the rod; in the latter mode (Scheme S1(b)), the carboxylato groups synchronously connect with the Dy1 and $Dy2^{i}$ (^{i} −1+x, y, z) atoms or the $Dy1^{ii}$ (^{ii} x, 1+y, z) and $Dy2^{iii}$ (^{iii} −1+x, 1+y, z) atoms as a bismonodentate bidentate ligand, and the $Dy_2(CO_2)_4$ paddle-wheel units are linked together by couples of such ligands to form the Dy_4L_2 loops and extended 1D tape structure along the *b*-axis direction. The coordination-unsaturated $Dy_2(CO_2)_4$ paddle-wheel units from the neighbouring tapes are further connected with each other by the rod ligands, resulting in the 2D network.

The most amazing structural feature of **1** is that two such 2D networks weave in a 2D→2D parallel way, creating a 2D polyrotaxane layer (Fig. 1c). The Dy_4L_2 loops of each net are penetrated by the rod ligands from the other net, therefore, both polyrotaxane and polycatenane characters are presented in such an unusual interlocked 2D sheets (Fig. 1d), which can be topologically described by the 6-connected ($2^2 \cdot 4^8 \cdot 6^5$) nets rather than the 4-connected (4,4) nets. This kind of interpenetrating network is still quite rare, and only several transition metal systems with the same entanglement topology are known.[8] In addition, the interlocked nets of **1** are stabilized by both intranet and internet hydrogen bonds.

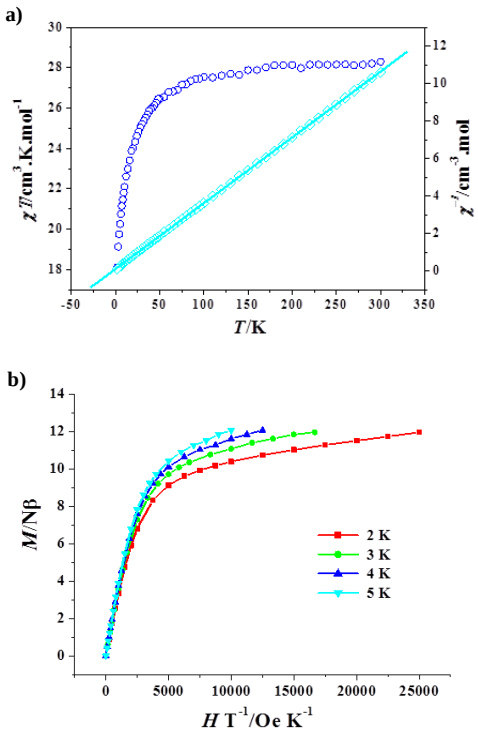

Fig. 2. (a) Plots of χT versus T (○) and $1/\chi$ versus T (◊) of complex **1**, the solid line represents the best theoretical fitting; and (b) M versus H/T plots at temperatures below 5 K.

Direct-current (dc) magnetic susceptibility studies of **1** indicated that the room temperature χT value of 28.29 cm^3Kmol^{-1} is in good agreement with the theoretic value of 28.34 cm^3Kmol^{-1} for two uncoupled Dy^{3+} ions (S = 5/2, L = 5, $^6H_{15/2}$, g = 4/3) (Fig. 2a). Upon cooling, the χT product becomes small gently until 50 K and then falls rapidly, reaching a minimum value of 18.10 cm^3Kmol^{-1} at 2 K. The susceptibility data could be fitted to the Curie–Weiss law, giving the Curie constant C of 28.51 cm^3Kmol^{-1} and the Weiss constant θ of −3.40 K. The small negative θ value suggests that the decline of the χT value with decreased temperature mainly comes

from the magnetic anisotropy and the thermal depopulation of the Dy^{3+} excited states (Stark sublevels of the $^6H_{15/2}$ state). The field dependence of the magnetization at different temperatures revealed a rapid increase of magnetization at low magnetic fields but without any sign of saturation. The non-superimposed *M* versus *H/T* curves indicated the significant magnetic anisotropy and/or low-lying excited states (Fig. 2b).

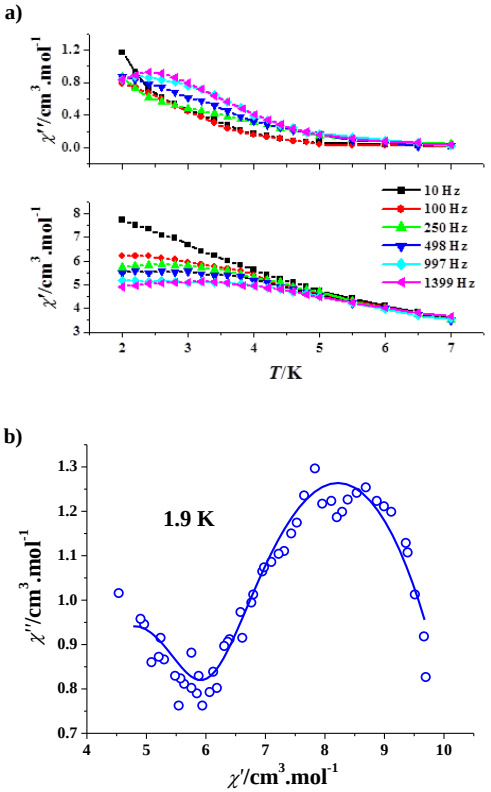

Fig. 3. (a) AC susceptibilities measured in a 2.5 Oe ac magnetic field with a 2 kOe dc-field for **1**; and (b) Cole–Cole plot at 1.9 K for **1** (H_{dc} = 2 kOe and H_{ac} = 2.5 Oe), the solid line represents the best fitting with the sum of two modified Debye functions.

Ac susceptibility measurements indicated that the out-of-phase susceptibilities of **1** are frequency-dependent at low temperature, but no peak could be observed (Fig. S3). Such a case is often observed for the pure 4f SMMs/SIMs and 3d-4f SMMs/SIMs,[2] because the magnetic relaxation process may be partially influenced by quantum tunnelling effects. After applying a dc field of 2000 Oe, some peaks could be observed in high-frequency region of the χ'' signals (Fig. 3a), which indicates that this dc field can effectively remove the ground state degeneracy, partly suppressing the quantum tunnelling effects. The shift of peak temperature (T_f) of the χ'' signals was assessed by the parameter, $\phi = (\Delta T_f/T_f)/\Delta(\log f)$, giving the value of 0.30. This ϕ value is in the normal range for a superparamagnet ($\phi >$ 0.1) but obviously larger than that for a spin glass state ($\phi \approx 0.01$),[9] implying the SMM behaviours of **1**. The oscillating frequencies corresponding to the peak temperatures were fit by the Arrhenius law, $\tau = \tau_0 \exp(U_{eff}/k_B)$, affording the U_{eff} value of 12.5 K and the τ_0 value of 6.0×10^{-7} s (Fig. S4). The τ_0 value is consistent with the normal SMM or SIM τ_0 values of 10^{-6}-10^{-11} s.[2,3]

More significant are the dynamic magnetic behaviours of **1** in the form of χ'' versus χ' plot (Fig. 3b). Interestingly, two separate relaxation processes were clearly observed in the Cole–Cole plot, corresponding to the fast relaxation phase (FR) and the slow relaxation phase (SR), respectively. The two-step relaxation process could be described by the sum of two modified Debye functions:[10,5b,5c,5e]

$$\chi_{ac}(\omega) = \frac{\chi_2 - \chi_1}{1 + (i\omega\tau_2)^{(1-\alpha_2)}} + \frac{\chi_1 - \chi_0}{1 + (i\omega\tau_1)^{(1-\alpha_1)}} + \chi_0 \quad (1)$$

The results are summarized in Table S1 and shown in Fig. 3b and Fig. S5. The α_1 value of 0.44 is larger than the α_2 value of 0.31, suggesting that the slow relaxation phase has a relatively narrow distribution of the relaxation time with respect to the fast one. The two-step relaxation process maybe is attributable to the existence of two types of Dy(III) coordination geometries(square antiprism and bicapped trigonal prism) in **1**. To the best of our knowledge, the two-step relaxation process has never been observed in the lanthanide–organic framework SMMs before,[4] although such a phenomenon is not unusual for the discrete pure 4f SMMs/SIMs.[2,5b,5c,10b] Additionally, the *M* versus *H* plot at 1.9 K does not show any hysteresis (Fig. S5).

In summary, the use of the semi-rigid V-shape dicarboxylate ligand has provided access to a 2D→2D polyrotaxane Dy(III) metal–organic framework, which shows slow magnetization relaxation of the SMM behaviours. This work demonstrates that, except the transition metal ions, the lanthanide ions also can act as the nodes to construct fantastic polyrotaxane metal–organic frameworks with interesting physical properties.

Acknowledgements

This work was supported by National Key Basic Research Program of China (2013CB933403), National Natural Science Foundation of China (91022014 and 21073198), and the Strategic Priority Research Program of the Chinese Academy of Sciences (XDB12010103).

Notes and references

[a] *Beijing National Laboratory for Molecular Sciences, Center for Molecular Science, Institute of Chemistry, Chinese Academy of Sciences, Beijing 100190, P. R. China; E-mail: cmliu@iccas.ac.cn*

† Electronic Supplementary Information (ESI) available: coordination modes of the L^{2-} ligands (Scheme 1s), X-ray crystallographic data for **1** in CIF format, TGA (Fig. S1), additional figures of the crystal structure (Fig. S2) and magnetic characterization(Fig. S3-S5 and Table S1). CCDC reference number 1009602. For crystallographic data in CIF or other electronic format see DOI: 10.1039/b000000x/

‡ Elemental analysis (%): Calc. for $C_{42}H_{34}Dy_2O_{23}S_3$ (**1**): C 37.99, H 2.58, N27.71; found: C 38.04, H 2.62, N 27.67. IR (KBr): *v*=3444(s, br), 1695(w), 1652(m), 1625(m), 1570(w), 1539(m), 1491(w), 1420(s), 1411(s), 1386(m), 1324(w), 1301(m), 1164(m), 1140(w), 1100(m), 1070(w), 1018(w), 860(w), 777(w), 738(m), 721(w), 691(w), 613(w), 574(w), 487(w), 437(w) cm^{-1}.

§ Crystal data: $C_{42}H_{34}Dy_2O_{23}S_3$, *M*r = 1327.90, monoclinic, $P2_1/c$, a = 17.772(4) Å, b = 12.695(3) Å, c = 22.095(9) Å, β = 119.79(2)°, V = 4326(2) $Å^3$, Z= 4, T = 173(2) K, D_{cal} = 2.039 g/cm^3, μ = 3.666 mm^{-1}, GOF = 1.193, $R1$ = 0.0582, $wR2$ = 0.1158 ($I > 2\sigma(I)$).

1 (a) S. R. Batten and R. Robson, *Angew. Chem. Int. Ed.*, 1998, **37**, 1460; (b) K. Kim, *Chem. Soc. Rev.*, 2002, **31**, 96; (c) L. Carlucci, G. Ciani and D. M. Proserpio, *CrystEngComm*, **2003**, *5*, 269; (d) N. W. Ockwig, O. Delgado-Friederichs, M. O'Keeffe and O. M. Yaghi, *Acc. Chem. Res.*, 2005, **38**, 176; (e) S. J. Loeb, *Chem. Commun*., 2005, 1511; (f) J. J. Perry IV, V. C. Kravtsov, G. J. McManus and

M. J. Zaworotko, *J. Am. Chem. Soc.*, 2007, **129**, 100762; (g) J. Yang, J.-F. Ma and S. R. Batten, *Chem. Commun.*, 2012, **48**, 7899.

2 (a) D. N. Woodruff, R. E. P. Winpenny and R. A. Layfield, *Chem. Rev.*, 2013, **113**, 5110; (b) P. Zhang, Y.-N. Guo and J. Tang, *Coord. Chem. Rev.*, 2013, **257**, 1728.

3 (a) R. Sessoli, D. Gatteschi, A. Caneschi and M. A. Novak, *Nature*, 1993, **365**, 141; (b) G. Christou, D. Gatteschi, D. N. Hendrickson and R. Sessoli, *MRS Bull.*, 2000, **25**, 66; (c) L. M. C. Beltran and J. R. Long, *Acc. Chem. Res.*, 2005, **38**, 325; (d) C. Benelli and D. Gatteschi, *Chem. Rev.*, 2002, **102**, 2369; (e) R. Bagai and G. Christou, *Chem. Soc. Rev.*, 2009, **38**, 1011; (f) G. E. Kostakis, A. M. Akoab and A. K. Powell, *Chem. Soc. Rev.*, 2010, **39**, 2238; (g) V. Chandrasekhar and B. Murugesapandian, *Acc. Chem. Res.*, 2009, **42**, 1047; (h) R. Sessoli and A. K. Powell, *Coord. Chem. Rev.*, 2009, **253**, 2328; (i) M. Murrie, *Chem. Soc. Rev.*, 2010, **39**, 1986; (j) T. Komeda, H. Isshiki, J. Liu, Y.-F. Zhang, N. Lorente, K. Katoh, B. K. Breedlove and M. Yamashita, *Nat. Comm.*, 2011, **2**, 217; (k) N. Ishikawa, M. Sugita, T. Ishikawa, S. Koshihara and Y. Kaizu, *J. Am. Chem. Soc.*, 2003, **125**, 8694; (l) S.-D. Jiang, B.-W. Wang, H.-L. Sun, Z.-M. Wang and S. Gao, *J. Am. Chem. Soc.*, 2011, **133**, 4730; (m) W.-X. Zhang, R. Ishikawa, B. Breedlove and M. Yamashita, *RSC Adv.*, 2013, **3**, 3772.

4 (a) D. Savard, P. H. Lin, T. J. Burchell, I. Korobkov, W. Wernsdorfer, R. Clerac and M. Murugesu, *Inorg. Chem.*, 2009, **48**, 11748; (b) P. F. Shi, Y. Z. Zheng, X. Q. Zhao, G. Xiong, B. Zhao, F. F. Wan and P. Cheng, *Chem.-Eur. J.*, 2012, **18**, 15086; (c) F. R. Fortea-Perez, J. Vallejo, M. Julve, F. Lloret, G. De Munno, D. Armentano and E. Pardo, *Inorg. Chem.*, 2013, **52**, 4777; (d)X. Yi, K. Bernot, G. Calvez, C. Daiguebonne and O. Guillou, *Eur. J. Inorg. Chem.*, 2013, 5879; (e) Q.-Y. Liu, Y.-L. Li, Y.-L. Wang, C.-M. Liu, L.-W. Ding and Y. Liu, *CrystEngComm*, 2014, **16**, 486.

5 (a) C.-M. Liu, D.-Q. Zhang, X. Hao and D.-B. Zhu, *Cryst. Growth& Des.*, 2012, **12**, 2948; (b) C.-M. Liu, D.-Q. Zhang and D. B. Zhu, *Inorg. Chem.*, 2013, **52**, 8933; (c) C.-M. Liu, D.-Q. Zhang and D. B. Zhu, *Dalton Trans.*, 2013, **42**, 15317; (d) C.-M. Liu, D.-Q. Zhang and D. B. Zhu, *Dalton Trans.*, 2010, **39**, 11325; (e) C.-M. Liu, D.-Q. Zhang, X. Hao and D.-B. Zhu, *Chem.-Asian J.*, 2014, **7**, 12345.

6 (a) C.-M. Liu, J.-L. Zuo, D.-Q. Zhang and D.-B. Zhu, *CrystEngComm*, 2008, **10**, 1674; (b) C.-M. Liu, M. Xiong, D.-Q. Zhang, M. Du and D.-B. Zhu, *Dalton Trans.*, 2009, 5666.

7 M. G. B. Drew, *Coord. Chem. Rev.*, 1977, **24**, 179.

8 (a) D. M. L. Goodgame, S. Menzer, A. M. Smith and D. J.Williams,*Angew. Chem. Int. Ed.*, 1995, **34**, 574; (b) Y.-Q. Lan, S.-L. Li, J.-S. Qin, D.-Y. Du, X.-L. Wang, Z.-M. Su and Q. Fu, *Inorg. Chem.*, 2008, **47**, 10600; (c) J. Yang, J.-F. Ma, S. R. Batten and Z.-M. Shu, *Chem.Commun.*, 2008, 2233; (d) F. Luo, Y.-T. Yang, Y.-X. Che and J.-M. Zheng, *CrystEngComm*, 2008, **10**, 981; (e) Y. Ma, A.-L. Cheng and E.-Q. Gao, *Cryst. Growth & Des.*, 2010, **10**, 2832; (f) Y.-Y. Liu, Z.-H. Wang, J. Yang, B. Liu, Y.-Y. Liu and J.-F. Ma, *CrystEngComm*, 2011, **13**, 3811.

9 J. A. Mydosh, *Spin Glasses, An Experimental Introduction*; Taylor and Francis: London, 1993.

10 (a) M. Grahl, J. Kotzler and I. Sessler, *J. Magn. Magn. Mater.*, 1990, **90-1**, 187; (b) Y.-N. Guo, G.-F. Xu, P. Gamez, L. Zhao, S.-Y. Lin, R. Deng, J. Tang and H.-J. Zhang, *J. Am. Chem. Soc.*, 2010, **132**, 8538; (c) S. K. Langley, N. F. Chilton, B. Moubaraki and K. S. Murray, *Inorg. Chem.*, 2013, **52**, 7183; (d) S. Das, A. Dey, S. Biswas, E. Colacio and V. Chandrasekhar, *Inorg. Chem.*, 2014, **53**, 3417; (e) J. Long, F. Habib, P.-H. Lin, I. Korobkov, G. Enright, L. Ungur, W. Wernsdorfer, L. F. Chibotaru and M. Murugesu, *J. Am. Chem. Soc.*, 2011, **133**, 5319. (f) R. J. Blagg, L. Ungur, F. Tuna, J. Speak, P. Comar, D. Collison, W. Wernsdorfer, E. J. L. McInnes, L. F. Chibotaru and R. E. P. Winpenny, *Nature Chem.*, 2013, **5**, 673.

